Respiratory bioaerosol deposition from a cough and recovery of viable viruses on nearby seats in a cabin environment

Short running title: **Bioaerosol deposition in a cabin**

C. T. Wang[1,2], J. C. Xu[2], S. C. Fu[1*], K. C. Chan[1], Christopher Y. H. Chao[1]

[1] Department of Mechanical Engineering, The University of Hong Kong, Hong Kong, China

[2] Department of Mechanical and Aerospace Engineering, The Hong Kong University of Science and Technology, Hong Kong, China

Corresponding email: scfu@hku.hk

Acknowledgements

The work was supported by the Collaborative Research Fund (CRF) project (no. C7025-16G) and the General Research Fund (no. 17203220) granted by the Research Grants Council of the Hong Kong Special Administrative Region, China.

Abstract

Respiratory bioaerosol deposition in public transport cabins is critical for risk analysis and control of contact transmission. In this work, we built a two-row four-seat setup and an air duct system to simulate a cabin environment. A thermal manikin on the rear left-hand seat was taken as the infected passenger (IP) and "coughed" three times through a cough generator. The deposited viruses and droplets on nearby seats were measured by a cultivation method and microscope, respectively. The effects of seat backrest and overhead gasper jet were studied. Results showed

that the number of deposited virus on the front seat was one order of magnitude higher than that on other seats which only contained droplets smaller than 10 μm in diameter. When the backrest was 15 cm higher than the cough, the deposited number of viruses was reduced to 5% of that with the backrest at the same height with the cough. The gasper jet above the IP with a velocity of 1.5 m/s can reduce the deposited viruses to 4% of that with gasper off. It indicates that both the gasper jet and backrest can work as mitigation measures to block the cough jet and protect the nearby passengers.

Keywords: Public transport; Cough; Deposition; Cabin environment; Gasper jet; COVID-19

Practical implications

- The high number of deposited viruses on the front seat area indicates that people should pay special attention on front seat in surface hygiene.
- The seat backrest can effectively block the cough jet and protect the passenger from direct exposure to cough jet, and the minimum height of the backrest should cover the passenger's head.
- The gasper jet can bend and prevent the cough jet from directly entering the regions of nearby passengers, so it is suggested to turn on all gasper jets in all passenger seats in order to mitigate infection risk.
- The reduction of bioaerosol deposition and the thermal comfort is possible to be fulfilled simultaneously by locating the gasper jet in the middle of the space between two rows of seats.
- The detailed distributions of viruses and droplets can be used to verify the computational fluid dynamics (CFD) models for short-range bioaerosol deposition and to evaluate the infection risk of contact route.

1 INTRODUCTION

Infectious disease transmission in public transportation (e.g. buses, trains, and airplane cabins) has attracted a lot of research interest [1-3]. Passenger cabin is an enclosed indoor environment with special geometric setup and high occupant density, which increase the risk of respiratory disease transmission, such as influenza, SARS, and COVID-19 [4,5]. Respiratory activities of infected passengers, e.g. cough, are initial sources of respiratory pathogens in a cabin environment. Released bioaerosols will be dispersed in the cabin and inhaled by other passengers and cause infections, and the transmission through this process is called airborne route. Some bioaerosols may directly deposit on the facial membranes of other passengers by spraying and cause infections, and this transmission process is called droplet route. There is also another transmission route called contact route which refers to the deposition of bioaerosols on surfaces in the cabin and transportation of the pathogens to the facial membranes by hand touching. The contact transmission is one of the important routes of respiratory disease transmission [6,7] and it can happen over the whole cabin by touching. Deposition of respiratory viruses was the first step of the contact transmission but was less studied. Understanding the respiratory bioaerosol deposition and distribution in a cabin environment is critical for surface hygiene and mitigating the infectious disease transmission.

The deposition of cough droplets highly depends on the cough jet dynamics. For a cough jet, the released cough droplets firstly travel forward as a jet with large momentum and high number concentration [8-10]. Large droplets quickly deposit on nearby surfaces (within around 2 m) because of the large gravitational and inertial forces, while smaller airborne droplet nuclei can disperse further away following background airflows with decreasing number concentration [11]. Therefore, in a cabin environment, the deposition on seats far away from the source should be mainly from

the airborne droplet nuclei. Many researchers have focused on modelling the airborne aerosol deposition on indoor surfaces [12-18]. For nearby seats within 1-2 m of the infected passenger, the deposition should be mainly from the inertial impaction due to the large inertial force. It will result in high volume of respiratory fluid on nearby surfaces, indicating a higher infection risk to passengers compared with the seat far away. Thus, a detail study on the bioaerosol deposition and distribution on nearby seats is essential.

Much research has been done about the respiratory aerosol dispersion in public transport cabins. Many works were conducted in aircraft cabins. Zhang and Chen (2007) [19] investigated the effect of mixing ventilation, under-floor displacement ventilation, and a personalized ventilation on transporting contaminant. Sze-To et al. (2009) [20] and Gupta et al. (2011) [21] studied cough droplet temporal and spatial dispersion. Some works studied aerosol dispersion in trains. Zhang and Li (2012) [22] studied cough droplet dispersion under four different ventilation conditions in a high-speed rail cabin. Yang et al. (2018) [23] studied the effect of diffuser types on contaminant transport in a high-speed train cabin. Some studies were conducted in buses or cars. Zhu et al. (2012) [24] investigated airborne aerosol transportation under three mixing ventilations and a displacement ventilation. Yang et al. (2020) [25] studied respiratory droplet dispersion pattern in a coach bus under different diffuser directions, relative humidity, and droplet sizes. Mathai et al. (2021) [26] studied aerosol transportation between the driver and passenger in a car and evaluated the effect of windows on the dispersion of aerosols. Above mentioned studies mainly focused on airborne droplet nuclei dispersion in the whole cabin and the bioaerosol deposition was not involved. Sze-To et al. (2009) [20] and Wan et al. (2009) [27] studied both the cough droplet dispersion and deposition in an aircraft cabin mock-up. They measured the overall deposition fraction on each seat and passenger but the detailed droplet distribution on nearby seats, such as the highly touched surface

of top surface of a seat backrest and head area of the passenger, is yet to be studied. Furthermore, some parameters in cabins, such as the seat setup and overhead gasper jet, can also affect the bioaerosol deposition on nearby surfaces but have not been considered in their studies.

In different cabin environments, the relative height between seated passengers and seat backrests varies, and the distance between two seat rows is also different. When the relative height changes, the backrest may partially or fully block the cough jet. The relative distance between two seat rows also affects the impaction of cough jet and deposition of bioaerosols. Wang et al. (2020) [28] studied the bioaerosol deposition from a cough on a front plate with different relative angles and distances. They identified the impaction region on the front plate with high bioaerosol concentration and suggested that the plate can block the cough jet and protect people behind. The setting of the front plate is analogous to a seat backrest, thus their result provides the base in studying the deposition of bioaerosol on backrests in a cabin. However, it is possible that the cough jet by-passes the backrest causing bioaerosol deposition on the passengers behind. Therefore, the effect of seat arrangement on deposition of bioaerosol on nearby seats and passengers is important for the infection control in a cabin environment but remains unknown.

Gaspers are typically installed above passengers' seats to provide proper thermal condition in cabin environments. The flow rate and direction of the gasper are, sometimes, adjustable by the passengers. The gasper jet can directly interact with the cough jet and affect the droplet deposition. Guo et al. (2014) [29], Dai et al. (2015) [30], and Shi et al. (2016) [31] studied the flow characteristics of the gasper jet such as velocity profile and turbulence intensity in a cabin. Li et al. (2018) [32] studied the effect of the main ventilation on the gasper jet by particle image velocimetry. Li et al. (2015) [33] investigated the effect of the gasper jets on thermal environment and contaminant transport (i.e. tracer gas). These studies indicated the dominant effect of gasper jet on surrounding environment.

However, the effect of gasper jet on cough jet, which has the same order of magnitude of the gasper jet, has not been studied yet. The gasper jet in public transport cabins can be regarded as a personalized ventilation. Researchers found that a well-designed personalized ventilation can effectively block the cough droplets and protect the user [34-37]. The overhead gasper nozzle diameter is around 1.8 cm for aircraft cabin and around 5 cm for buses, which are much smaller than the diameter (e.g. 10 cm) of a well-designed personalized ventilation. The performance of the overhead gasper jet on reducing bioaerosol deposition and protecting passengers is unknown.

In this work, a two-row four-seat setup together with an air duct system were built in a conditioned room. Cough was chosen as the bioaerosol source because it is a violent respiratory activity that releases numerous high velocity bioaerosols and there is a high risk to contaminate the nearby surface by deposition. The purposes are to investigate the bioaerosol deposition and distribution from a cough on nearby seats and study the effects of seat geometric setup (height of backrest and distance between two rows) and overhead gasper jet (velocity, position, and status of open or closed). Bacteriophage T3 was added into artificial saliva solution to represent respiratory viruses. Number concentration of recovered virus and deposited droplet was measured to characterize the deposition on nearby seats and passengers.

2 MATERIALS AND METHOD

2.1 Experimental setup and studied cases

Four seats and four identical seated thermal manikins, as shown in Fig. 1a, were prepared and located in a conditioned room with temperature of 20ºC ± 1ºC and relative humidity of 67% ± 4%. The relative humidity was close to the real condition of trains and buses, but it was higher than the average relative humidity of 17.9%-27.0% in aircraft cabins [38]. Top view of the tested room was

shown in Fig. 1b. The outlet was located at the lower area of side wall. The two inlets were located at ceiling. The size of the room was 8.7 m × 2.9 m × 3.7 m (L × W × H). Background airflow velocity at the area of the experimental setup was less than 0.1 m/s measured by a flow meter (7575-X, Q-track, TSI, USA). The manikin at the rear left-hand seat was considered as the infected passenger (IP). The other three manikins were considered as the healthy passenger (HP). The manikin at the front left-hand seat was denoted as HP_1. The manikin at the front right-hand seat was denoted as HP_2. The manikin at the rear right-hand seat was denoted as HP_3, as shown in Fig. 1a. A cough generator was installed in the mouth of the IP to simulate coughing processes. It was the same one used in our previous work [28]. The releasing velocity of cough droplets was around 12 m/s which is similar to the average cough droplet velocity of 11.7 m/s. The size distribution was similar to a real cough with the peak size of 10-20 μm [39]. Backrests of the four seats were made from polyfoam with width of 45 cm and thickness of 11 cm. A 1 cm gap was left between the backrests in the same row. An air duct system was built and put above the passengers. It has four identical gaspers with a nozzle diameter of 5 cm which were the same as that used in buses as shown in Fig. 1a.

Four relative heights of backrest, *H,* were studied: -15, 0, 15, and 30 cm, for which the value was compared with the height of the IP's mouth. The *H* of 15 cm meant that the backrest was 15 cm higher than the mouth and just covered the whole head of the manikin. Three relative distances between the front backrest and the IP, *D,* were investigated: 20, 50, and 80 cm. Four velocities, *V*, of the IP's gasper jet were studied: 0, 0.75, 1.5, and 2.5 m/s. Two statuses of HP's gasper were denoted as 'open' and 'closed' with velocity *V* of 1.5 m/s and 0 m/s, respectively. The velocities of the IP's and HP's gasper jet were measured beneath the gasper with the same height as the cough, as shown in Fig. 1b. The IP's gasper can be moved back and forth at the same height and the gasper

jet was always directly downward at a 90º angle for studied cases. Three locations were studied: near the HP, in middle, near the IP as shown in Fig. 1b. In total, five parameters including 13 cases were studied, as listed in Table 1. The cases 1, 2, 3, and 4 focus on the effect of *H*; cases 2, 5, and 6 focus on the effect of *D*; cases 2, 7, 8, and 9 focus on the effect of *V*; cases 2, 8, 10, and 11 focus on the effect of the position of the IP's gasper jet; cases 2, 11, 12, and 13 focus on the effect of the status of the IP's and HPs' gasper (open or closed).

2.2 Experimental procedure and schematic diagram of sampling

In the experiment, the IP 'coughed' 3 times with a time interval of 5 second, and each cough lasted 1 second (releasing 0.075 mL artificial saliva solution). Then the cough droplets travelled forward together with the cough air jet. The larger droplets can maintain spherical shape in liquid status and deposit on nearby surfaces. The smaller droplets became droplet nuclei and may deposit or suspend in air. After the deposition and sample collection, one part of the sample with size of 1 cm × 5 cm or 1 cm × 11 cm was cut for inspection using a microscope (Ni-E, Nikon, Japan) to obtain the number concentration of deposited droplets. A microscopy method similar to our previous work was employed [28]. The droplets on pictures were automatically identified and counted by the software of the microscope. The contact diameter of the droplets was measured to indicate the droplet's size. The PVC samples for experiment were kept clean to avoid the contamination of deposited droplets. The other part of the sample was dipped into a tube with 5 mL sterilized water to extract the deposited viruses from the surface. Then, the solution was diluted by serial dilution method. The viable virus concentration in each diluted solution was then measured by top layer agar method, which was described in detail in Section 2.3.

The sampling area was divided into top surface of backrests, head surface of passengers, and back surface of backrests. The sampling point and abbreviation of each point were shown in Fig. 1 and

Table 2, respectively. Polyvinyl chloride (PVC) plates with thickness of 0.6 mm were attached on the sampling positions. Samples with size of 11 cm × 5 cm and 5 cm × 5 cm were used for the sampling as shown in Fig. 2b.

2.3 Artificial saliva solution preparation and viable virus enumeration

Artificial saliva solution consists of 12 g sodium chloride and 76 g glycerol in 1 L sterilized water, which has been used in references [28,40]. Non-volatile material in the solution accounts for 6% in volume, similar with the real human saliva [41]. Bacteriophage T3 (ATCC 11303 B3) was used to represent the respiratory viruses. High-titer phage solution of 100 μL (up to $10^{10\text{-}11}$ PFU/ mL) was mixed with around 200 mL artificial saliva solution. The final phage concentration in the saliva solution for cough generator was around 10^7 PFU/mL. The method of preparing high-titer phage solution can be found in references [28,42].

The top agar layer method was used to measure viable phage number concentration in solutions. Agar plates were first prepared in advance. Phage solution of 0.2 mL was mixed with its host *Escherichia coli* (*E. coli*) solution of 0.2 mL in a tube. After waiting 15 minutes for the phage to attack its host *E. coli* cell, the solution was then mixed with 3 mL 52 ºC melted soft agar [in g/L: nutrient broth, 25; agar powder, 7], and poured onto the prepared agar plate. The double-layer agar plates were then put into an incubator for 6 h with temperature of 37 ºC. The plaque-forming unit (PFU) on the plate was then counted and the phage concentration was calculated based on PFU number and dilution ratio of the solution.

2.4 Normalized PFU at six sampling areas

To quantitatively compare the effect of the five parameters on reducing the deposition, PFU on each area was normalized to PFU on that area of Case 2, in which H = 0 cm, D = 50 cm with gaspers closed.

$$Normalized\ PFU = \frac{PFU\_area}{PFU\_area\ of\ case\ 2} \quad (1)$$

In each area of BS_1, TS_1, HS_1, BS_2, TS_2, and HS_2, the PFU_area was the mean PFU value of the sampling points of that area. The $Normalized\ PFU$ indicates the effect of studied parameters for each area compared with Case 2.

3 RESULTS

3.1 Bioaerosol distribution on nearby seats and passengers with the IP's and HP's gasper closed

Fig. 3a shows the detailed viable virus distribution on sampling points of Case 2 with H = 0 cm, D = 50 cm with gaspers closed. The backrest had the same height as the cough and partially block the cough jet. The peak PFU value happened on the back surface of HP_1's backrest (i.e. point $\mathbf{a_1}$) which was directly facing the cough jet. The PFU value decreased greatly from point $\mathbf{a_1}$ to point $\mathbf{c_1}$ on the backrest. Moreover, the PFU value at point $\mathbf{a_1}$ of the back surface was around six times of that on point $\mathbf{m_1}$ of the top surface, although two points have similar distance with the cough source. It is because the plane of point $\mathbf{a_1}$ was in perpendicular to the cough jet while the plane of point $\mathbf{m_1}$ was in parallel to the cough jet, indicating different deposition mechanisms. It was found that the PFU value on top surface decreased gradually from point $\mathbf{m_1}$ to point $\mathbf{r_2}$.

Fig. 3b shows the mean PFU value for the area of BS_1, TS_1, HS_1, BS_2, TS_2, and HS_2. It shows that the PFU value decreased from back surface to top surface and then to head area for both HP_1 and HP_2. The PFU value in each area of Case 2 will be used to normalize the PFU value at that area of

different cases and to indicate the effect of studied parameters in the following Sections. Fig. 3c shows the PFU value on HP_1 and HP_2. It indicated that the PFU on HP_1 was one magnitude order higher than that on HP_2.

Fig. 3d shows the detailed droplet number distribution of Case 2 with five size channels. By comparing the PFU value with droplet distribution in Fig. 3a and 3d, it is found that the high PFU areas matched with the areas containing large portion of droplets with large droplet size (diameter larger than 10 μm), such as the points **a_1-c_1, m_1,** and **n_1**. The low PFU areas matched with the areas only containing droplets smaller than 10 μm in diameter, such as the points **l_2-m_4**, **f_2**, **h_2**, and **n_2**. In addition, the areas of HP_2 only contained the droplets smaller than 10 μm, indicating that the large cough droplets directly deposit on the front seat and only some airborne droplets can disperse to and deposit on the area of HP_2.

3.2 Effect of relative height H of backrest on bioaerosol distribution

Fig. 4 shows the viable virus distribution on nearby seats under four relative heights of the backrest. When H = -15 cm, cough jet travelled above the backrest. The high PFU value appeared at the top surface and neck of the $_{HP1}$ which were directly exposed to the droplet jet without the block of backrest. PFU on the back surface was relatively lower. When H = 0 cm, the backrest had the same height with the cough and partially blocked the cough jet. The peak PFU value happened on the back surface and top surface of HP_1's backrest which were directly facing the cough jet. When H = 15 or 30 cm, the backrests were 15 or 30 cm higher than the cough and blocked the cough jet. There was almost no viable virus on the top surface and head area of both HP_1 and HP_2. The PFU value on the back surface (i.e. point **a_1**, **b_1**, **c_1**, and **a_2**) was not reduced as the increase of backrest height and was much higher than that on the other areas. For the low PFU area of the top surface and head area, deposited droplets were found mainly smaller than 10 μm in diameter with a

relatively low and uniform number concentration, as shown in Figure 1S in Supplementary Information. It indicates that the large droplets in cough jet cannot bypass the backrest which blocks most of the large droplets and some airborne droplets from entering the front row.

Fig. 5 shows the effect of backrest height on virus deposition at six areas of HP_1 and HP_2. For H1 and H2, the normalized PFU was reduced linearly as the increase of the height from -15 cm to 15 cm, and the value was almost unchanged as it further increased to 30 cm. For TS_1 and TS_2, the normalized PFU was first increased and then decreased, and then it slightly decreased as the height further increased from 15 cm to 30 m. For TS1, when the height was increased to 15 cm, the backrest already blocked the cough jet, and it reduced the PFU to around 5% of that of Case 2. For BS_1 and BS_2, the normalized PFU was almost continuously increased as the height increased from -15 cm to 30 cm. It means that more viruses or droplets were directly deposited on the back surface as the increase of the height.

3.3 Effect of relative distance D on bioaerosol distribution

The PFU distributions on the nearby seats at three different relative distances (D = 20, 50, and 80 cm) were similar, but the PFU values decreased with the increase of D. The magnitude of peak PFU on the back surfaces decreased from 1200 to 600 and to 120 #/cm^2 when D increased from 20 to 50 and to 80 cm. The distributions of droplet number concentrations for D = 20, 50 and 80 cm were also similar. The highest number concentration on the back surface was reduced from ~3.5×10^4 to ~1.5×10^4 and to ~6×10^3 #/cm^2 when D increased from 20 to 50 and to 80 cm. The detailed distributions for different distances were shown in Figure 2S and 3S in Supplementary Information.

Fig. 6 shows the effect of the distance between two rows on virus deposition at the six areas of HP_1 and HP_2. For the BS_1 and TS_1, the normalized PFU was almost linearly decreased as the increase of the distance. For HS_1, the normalized PFU was decreased greatly and then decreased slightly as the height increased from 20 cm to 50 cm and to 80 cm. For the BS_2, TS_2, and HS_2, the normalized PFU was first increased and then decreased as the increase of the distance.

3.4 Effect of 'open' or 'closed' status of $_{HP}$'s and IP's gasper jets on bioaerosol distribution

Fig. 7 shows the viable virus number concentration and distribution on nearby seats under the 'open' or 'closed' status of IP's and HP's gaspers. When IP's gasper jet was closed, by comparing the upper-left panel and upper-right panel of Figure 7, it was found that the HP's gasper jet reduced PFU value on all sampling points except for the neck of HP_1 (i.e. point $\mathbf{n_1}$). When the IP's gasper was open (lower panels of Figure 7), the PFU values of all sampling points were reduced greatly, regardless of the HP's gasper being open or closed. Moreover, it was found that the droplets on the top surface and the head area were mainly the droplets smaller than 10 μm in diameter, as shown in Figure 4S in Supplementary Information. It indicates that the IP's gasper jet can effectively block most of the large droplets from the cough jet, while the HP's gasper jets did not directly interact with the cough jet and did not have much effect on reducing the deposition.

Fig. 8 shows the effect of the status of IP's and HP's gasper on virus deposition at the six areas of HP_1 and HP_2. It is found that once the IP's gasper was open, the normalized PFU values were similar for all six areas with a mean value of around 0.04, indicating that the IP's gasper jet can greatly reduce the bioaerosol deposition on nearby surfaces. When HP's gasper was open with IP's gasper being closed, the normalized PFU values varied for different areas. For HS_1, the normalized PFU was around 3.2, meaning that the HP's gasper enhanced the deposition on HP1's head area.

For BS_1, TS_1, and HS_2, the normalized PFU values were around 0.7. For BS_2 and TS_2, the normalized PFU was around 0.15.

3.5 Effect of IP's gasper position on bioaerosol distribution

When the IP's gasper was open and near the front HP_1, the PFU values on the sampling points were reduced compared with that with IP's gasper being closed. When the IP's gasper was in the middle or near the IP, the PFU was further reduced, as shown in Figure 5S in Supplementary Information. For the top surface and head area, the sizes of the deposited droplets were mainly smaller than 10 μm in diameter, as shown in Figure 6S in Supplementary Information. For the back surface of the HP_1's backrest, the peak PFU value decreased from ~400, to ~80 and to ~40 PFU/cm^2 as the IP's gasper was changed from 'Near HP' to 'In middle' and to 'Near IP'. Meanwhile, the peak PFU position on the back surface also gradually moved downward from position $\mathbf{a_1}$ to $\mathbf{e_1}$.

Fig. 9 shows the effect of the position of IP's gasper on virus deposition at the six areas of HP_1 and HP_2. It is found that when the IP's gasper was near the HP, the normalized PFU for six areas was different and varied from 0.05 to 0.61. For the area of HS_1, BS_2, and HS_2, the normalized PFU was smaller than 0.2, showing good protection ability for the head surfaces of front passengers. When it was in the middle, the normalized PFU for all six areas was substantially reduced with a mean value of 0.04. When it was near the IP, the normalized PFU was further and slightly reduced.

3.6 Effect of IP's gasper jet velocity V on bioaerosol distribution

When *V* was increased from 0 to 0.75 m/s, the PFU values on the sampling points were reduced, but the PFU distributions were similar. When *V* increased to 1.5 or 2.5 m/s, there was almost no PFU on the top surface and head area of both HP_1 and HP_2, and the droplets were mainly smaller than 10 μm in diameter, as shown in Figure 7S and 8S in Supplementary Information. For the back

surface, the peak PFU value decreased continuously from around 600 to 200 to 80, and to 20 PFU/cm^2 as V increased from 0 to 2.5 m/s. The peak position of PFU on the back surface gradually moved downward from point $\mathbf{a_1}$ to $\mathbf{b_1}$, indicating that the gasper jet can bend the cough jet downward gradually as the increase of the gasper jet velocity.

Fig. 10 shows the effect of the velocity of IP's gasper jet on virus deposition at the six areas of HP_1 and HP_2. It is found that as the increase of the velocity, the normalized PFU for all six areas decreased exponentially, indicating that the velocity of IP's gasper jet has similar effect for the areas of HP_1 and HP_2. The normalized PFU was fitted by an exponential equation ($Normalized\ PFU = e^{a \cdot V}$), where a was -1.403, -2.158, -2.332, -2.803, -1.922, and -2.606 for BS_1, TS_1, HS_1, BS_2, TS_2, and HS_2, respectively. When the velocity was 0.75, 1.5, and 2.5 m/s, the mean values of the normalized PFU for all six areas were around 20%, 4%, and 2%, respectively. It means that the velocity of 1.5 m/s was large enough to reduce most of the deposited virus.

4 DISCUSSION AND IMPLICATIONS

During current COVID-19 pandemic, SARS-CoV-2 viruses had been detected both in air [43] and on surfaces [44] from the environment occupied by COVID patient. Public transport cabins are high risk places of respiratory disease transmission, while contact transmission was less studied compared with the airborne transmission. The virus concentration on nearby seats is critical for risk assessment and control. To the best of our knowledge, this study is the first to quantify the detailed virus and droplet distributions on nearby seats and passengers in a cabin environment and study the effect of geometric setup and overhead gasper jet. For risk analysis of contact route, previous studies usually assumed that the respiratory virus is uniformly distributed on surfaces near the source [45,46], because of the lack of detailed data on virus distribution. The detailed concentration and distribution of viable viruses and droplets in this work can be used and provide the foundation

for conducting the risk analysis of contact transmission. In addition, computational fluid dynamics (CFD) simulation is an efficient method to obtain detailed bioaerosol distribution, while the experimental data of inertial deposition of cough droplets for CFD verification is lacking. Thus, the experimental data in this work can be helpful in verifying CFD models.

The surfaces on the front seat of HP_1 contain droplets or droplet nuclei of both sizes larger and smaller than 10 μm in diameter, while the seats of HP_2 and HP_3 mainly contain droplet nuclei of smaller than 10 μm in diameter, and their number concentrations are also much smaller than that on HP_1. Thus, it is reasonable to conclude that for the seats further away from the IP, the deposited droplet nuclei should be mainly smaller than 10 μm in diameter, and the deposited virus number should be much smaller than that on nearby seats. For cleaning and disinfection, people should pay special attention to the seats in front of infected passengers.

In public transport cabins, mixing ventilation strategy is commonly used. The mean flow velocity at the area around the passengers is low and thus has limited effect on the cough jet which has a relatively higher momentum. The passengers in front of a cough jet will directly be exposed to the bulk flow of the cough jet. In this work, it is found that the backrest, serving as a partition, can effectively block the cough jet and reduce the deposition on the front passengers. When the backrest is 15 cm higher than the cough, the deposition on head and top surface was reduced to 5% of that with that same height with the cough. The deposition reduction of the head area means that the infection risk via contact by hand touching is reduced. The deposition reduction of the top surface also reduces the contact transmission risk because when other passengers walk in the aisle, they will receive less viruses by holding the top surface of the backrest. Therefore, it is suggested that the backrest should be higher than the cough, and the height of 15 cm (i.e. the same height with the head) was the minimum height to block the cough jet in a cabin environment. Although a larger

amount of cough droplets will directly deposit on the back surface of the backrest, it does not pose a higher infection risk because it is not a frequently touched area, but regular disinfection is still needed.

The IP's gasper jet can bend the cough jet and effectively reduce bioaerosol deposition, which is an additional function except for providing thermal comfort. The IP's gasper jet can reduce the deposition to around 4% of that without the gasper jet, independent of the condition of other HPs' gasper jets. Since some diseases, e.g. COVID-19 can be spread by infected people even they have no symptoms, it is suggested to turn on all gasper jets in all passenger seats. Moreover, this work finds that the IP's gasper jet blowing downward in the middle between the front backrest and the IP, can achieve similar reduction effect to that blowing at the face of the IP. It is possible to adjust the gasper jet location and orientation in order to compromise between infection mitigation and thermal comfort.

There are some limitations of this work. The flow due to background ventilation was supposed to be negligible and the effects of movement of passengers was not studied. The gasper diameter varies in different public transport cabins and gasper jet orientation is adjustable by passengers. In this work we only considered the gasper with a diameter of 5 cm with jet blowing downward, and further studies are recommended. In addition, infectious viruses can also be detected from speaking or breathing aerosols, indicating the importance of breathing or speaking as the respiratory virus source [47-49]. Breathing droplets have lower releasing velocity and smaller size than cough droplets. Thus, the deposition and control measures for breathing droplets should be different from the cough droplet deposition and further studies are needed. Furthermore, the relative humidity considered in this work was 67% which was close to the environments of trains and buses, but higher than that in aircraft cabins. Special attention should be paid in applying the current result because a higher

relative humidity may result in the overestimation of the inertial deposition due to the smaller evaporation rate. Finally, wearing a mask would affect cough jet and change the infectious virus deposition. Further studies are needed to reveal the effect of wearing a mask on infectious virus deposition.

5 CONCLUSIONS

In this work, bioaerosol deposition on nearby seats from a cough in a cabin environment was studied. The effect of the seat setup and gasper jet on bioaerosol deposition was also quantified. The deposited virus number on front seat is one order of magnitude higher than that on other nearby seats. The front seat surfaces contain both large and small bioaerosols, while other seats only contain the bioaerosols smaller than 10 μm in diameter. Both the backrest and gasper jet can block the cough jet and greatly reduce the deposition on nearby surfaces. They can be mitigation measures against COVID-19 in a cabin environment.

DATA AVAILABILITY STATEMENT

The data that supports the findings of this study are available in the supplementary material of this article

CONFLICT OF INTEREST STATEMENT

No conflict of interest declared.

AUTHOR CONTRIBUTION STATEMENT

C.T. Wang: Experiment design; Conducting experiment; Data analysis; Original draft and editing. **J.C. Xu**: Experiment design; Experiment preparation; Review and editing. **S.C. Fu**: Conceptualization; Data analysis; Review and editing; Supervision. **K.C. Chan**: Experiment

design; Review and editing. **Christopher Y.H. Chao**: Conceptualization; Funding acquisition and resources; Supervision; Project administration.

SUPPORTING INFORMATION

The Supporting Information file includes additional information of the results of distribution of deposited cough droplets and viable viruses on nearby seats and passengers.

REFERENCES

1. Andrews JR, Morrow C, Wood R. Modeling the role of public transportation in sustaining tuberculosis transmission in south africa. Am J Epidemiol. 2013;177(6):556-561.

2. Browne A, St-Onge Ahmad S, Beck CR, Nguyen-Van-Tam JS. The roles of transportation and transportation hubs in the propagation of influenza and coronaviruses: A systematic review. J Travel Med. 2016;23(1):tav002.

3. Hertzberg VS, Weiss H, Elon L, Si W, Norris SL, FlyHealthy Research Team. Behaviors, movements, and transmission of droplet-mediated respiratory diseases during transcontinental airline flights. Proc Natl Acad Sci USA. 2018;115(14):3623-3627.

4. Troko J, Myles P, Gibson J, et al. Is public transport a risk factor for acute respiratory infection? BMC Infect Dis. 2011;11(1):16.

5. Shen J, Duan H, Zhang B, et al. Prevention and control of COVID-19 in public transportation: Experience from china. Environ Pollut. 2020:115291.

6. Killingley B, Nguyen-Van-Tam J. Routes of influenza transmission. Influenza Other Respir Viruses. 2013;7:42-51.

7. Rheinbaben FV, Schünemann S, Gross T, Wolff MH. Transmission of viruses via contact in ahousehold setting: Experiments using bacteriophage φX174 as a model virus. J Hosp Infect. 2000;46(1):61-66.

8. Xie X, Li Y, Chwang A, Ho PL, Seto WH. How far droplets can move in indoor environments–revisiting the wells evaporation–falling curve. Indoor Air. 2007;17(3):211-225.

9. Wei J, Li Y. Enhanced spread of expiratory droplets by turbulence in a cough jet. Build Environ. 2015;93:86-96.

10. Liu L, Wei J, Li Y, Ooi A. Evaporation and dispersion of respiratory droplets from coughing. Indoor Air. 2017;27(1):179-190.

11. Tang JW, Li Y, Eames I, Chan P, Ridgway GL. Factors involved in the aerosol transmission of infection and control of ventilation in healthcare premises. J Hosp Infect. 2006;64(2):100-114.

12. Lai AC, Nazaroff WW. Modeling indoor particle deposition from turbulent flow onto smooth surfaces. J Aerosol Sci. 2000;31(4):463-476.

13. Lai AC, Chen FZ. Comparison of a new eulerian model with a modified lagrangian approach for particle distribution and deposition indoors. Atmos Environ. 2007;41(25):5249-5256.

14. Chen F, Lai AC. An eulerian model for particle deposition under electrostatic and turbulent conditions. J Aerosol Sci. 2004;35(1):47-62.

15. Zhao B, Zhang Y, Li X, Yang X, Huang D. Comparison of indoor aerosol particle concentration and deposition in different ventilated rooms by numerical method. Build Environ. 2004;39(1):1-8.

16. Zhao B, Wu J. Particle deposition in indoor environments: Analysis of influencing factors. J Hazard Mater. 2007;147(1-2):439-448.

17. Chen F, Simon CM, Lai AC. Modeling particle distribution and deposition in indoor environments with a new drift–flux model. Atmos Environ. 2006;40(2):357-367.

18. Chao CYH, Wan MP, Sze To GN. Transport and removal of expiratory droplets in hospital ward environment. Aerosol Sci Tech. 2008;42(5):377-394.

19. Zhang T, Chen QY. Novel air distribution systems for commercial aircraft cabins. Build Environ. 2007;42(4):1675-1684.

20. Sze To GN, Wan MP, Chao C, Fang L, Melikov A. Experimental study of dispersion and deposition of expiratory aerosols in aircraft cabins and impact on infectious disease transmission. Aerosol Sci Tech. 2009;43(5):466-485.

21. Gupta JK, Lin C, Chen Q. Transport of expiratory droplets in an aircraft cabin. Indoor Air. 2011;21(1):3-11.

22. Zhang L, Li Y. Dispersion of coughed droplets in a fully-occupied high-speed rail cabin. Build Environ. 2012;47:58-66.

23. Yang L, Li M, Li X, Tu J. The effects of diffuser type on thermal flow and contaminant transport in high-speed train (HST) cabins–a numerical study. Int J Vent. 2018;17(1):48-62.

24. Zhu S, Srebric J, Spengler JD, Demokritou P. An advanced numerical model for the assessment of airborne transmission of influenza in bus microenvironments. Build Environ. 2012;47:67-75.

25. Yang X, Ou C, Yang H, et al. Transmission of pathogen-laden expiratory droplets in a coach bus. J Hazard Mater. 2020;397:122609.

26. Mathai V, Das A, Bailey JA, Breuer K. Airflows inside passenger cars and implications for airborne disease transmission. Sci Adv. 2021;7(1):eabe0166.

27. Wan MP, Sze To GN, Chao C, Fang L, Melikov A. Modeling the fate of expiratory aerosols and the associated infection risk in an aircraft cabin environment. Aerosol Sci Tech. 2009;43(4):322-343.

28. Wang CT, Fu SC, Chao CY. Short-range bioaerosol deposition and recovery of viable viruses and bacteria on surfaces from a cough and implications for respiratory disease transmission. Aerosol Sci Tech. 2020:1-15.

29. Guo Y, Jiang N, Yao S, Dai S, Liu J. Turbulence measurements of a personal airflow outlet jet in aircraft cabin. Build Environ. 2014;82:608-617.

30. Dai S, Sun H, Liu W, Guo Y, Jiang N, Liu J. Experimental study on characteristics of the jet flow from an aircraft gasper. Build Environ. 2015;93:278-284.

31. Shi Z, Chen J, You R, Chen C, Chen Q. Modeling of gasper-induced jet flow and its impact on cabin air quality. Energy Build. 2016;127:700-713.

32. Li J, Liu J, Dai S, Guo Y, Jiang N, Yang W. PIV experimental research on gasper jets interacting with the main ventilation in an aircraft cabin. Build Environ. 2018;138:149-159.

33. Li B, Duan R, Li J, et al. Experimental studies of thermal environment and contaminant transport in a commercial aircraft cabin with gaspers on. Indoor Air. 2016;26(5):806-819.

34. Xu J, Fu S, Chao CY. Performance of airflow distance from personalized ventilation on personal exposure to airborne droplets from different orientations. Indoor Built Environ. 2020:1420326X20951245.

35. Pantelic J, Tham KW, Licina D. Effectiveness of a personalized ventilation system in reducing personal exposure against directly released simulated cough droplets. Indoor Air. 2015;25(6):683-693.

36. Gao NP, Niu JL. Personalized ventilation for commercial aircraft cabins. J Aircr. 2008;45(2):508-512.

37. Xu JC, Wang CT, Fu SC, Chan KC, Chao CY. Short-range bioaerosol deposition and inhalation of cough droplets and performance of personalized ventilation. Aerosol Sci Tech. 2021:1-14.

38. Giaconia C, Orioli A, Di Gangi A. Air quality and relative humidity in commercial aircrafts: An experimental investigation on short-haul domestic flights. Build Environ. 2013;67:69-81.

39. Chao CYH, Wan MP, Morawska L, et al. Characterization of expiration air jets and droplet size distributions immediately at the mouth opening. J Aerosol Sci. 2009;40(2):122-133.

40. Wang CT, Leung WT, Xu JC, Fu SC, Chao CY. Droplet detachment behavior from a rough hydrophilic surface. J Aerosol Sci. 2020;139:105469.

41. Effros RM, Hoagland KW, Bosbous M, et al. Dilution of respiratory solutes in exhaled condensates. Am J Respir Crit Care Med. 2002;165(5):663-669.

42. Kunkel SA, Azimi P, Zhao H, Stark BC, Stephens B. Quantifying the size-resolved dynamics of indoor bioaerosol transport and control. Indoor Air. 2017;27(5):977-987.

43. Lednicky JA, Lauzardo M, Alam MM, et al. Isolation of SARS-CoV-2 from the air in a car driven by a COVID patient with mild illness. *medRxiv*. 2021.

44. Razzini K, Castrica M, Menchetti L, et al. SARS-CoV-2 RNA detection in the air and on surfaces in the COVID-19 ward of a hospital in milan, italy. Sci Total Environ. 2020;742:140540.

45. Jones RM, Adida E. Influenza infection risk and predominate exposure route: Uncertainty analysis. Risk Anal. 2011;31(10):1622-1631.

46. Lei H, Li Y, Xiao S, et al. Routes of transmission of influenza A H1N1, SARS CoV, and norovirus in air cabin: Comparative analyses. Indoor Air. 2018;28(3):394-403.

47. Stelzer-Braid S, Oliver BG, Blazey AJ, et al. Exhalation of respiratory viruses by breathing, coughing, and talking. J Med Virol. 2009;81(9):1674-1679.

48. Yan J, Grantham M, Pantelic J, et al. Infectious virus in exhaled breath of symptomatic seasonal influenza cases from a college community. Proc Natl Acad Sci USA. 2018;115(5):1081-1086.

49. Patterson B, Wood R. Is cough really necessary for TB transmission? Tuberculosis. 2019;117:31-35.

Table 1. The studied cases and parameters

Case	Backrest height ***H*** (cm)	Relative Distance ***D*** (cm)	***V*** of IP's gasper jet (m/s)	Position of IP's gasper	Velocity of HP's gasper jet (m/s)
1	-15	50	0	Middle	0
2	0	50	**0 (i.e. closed)**	Middle	**0 (i.e. closed)**
3	15	50	0	Middle	0
4	30	50	0	Middle	0
5	0	20	0	Middle	0
6	0	80	0	Middle	0
7	0	50	0.7	Middle	0
8	0	50	1.5	Middle	0
9	0	50	2.5	Middle	0
10	0	50	1.5	Near HP	0
11	0	50	**1.5**	Near IP	**0 (i.e. closed)**
12	0	50	**0 (i.e. closed)**	Near IP	**1.5**
13	0	50	**1.5**	Near IP	**1.5**

Table 2. Abbreviations of sampling areas and points

TS_1	top surface of HP_1's backrest (mean of l_1, m_1, and r_1)	TS_2	top surface of HP_2's backrest (mean of l_2, m_2, and r_2)
HS_1	head surface of HP_1's backrest (mean of f_1, h_1, and n_1)	HS_2	head surface of HP_2's backrest (mean of f_2, h_2, and n_2)
BS_1	back surface of HP_1's backrest (mean of a_1, b_1, and c_1)	BS_2	back surface of HP_2's backrest (i.e. a_2)
l_1	left position of top surface of HP_1	l_2	left position of top surface of HP_2
m_1	middle position of top surface of HP_1	m_2	middle position of top surface of HP_2
r_1	right position of top surface of HP_1	r_2	right position of top surface of HP_2
f_1	face of HP_1	f_2	face of HP_2
h_1	head of HP_1	h_2	head of HP_2
n_1	neck of HP_1	n_2	neck of HP_2
a_1	upper point of back surface of HP_1	a_2	upper point of back surface of HP_2
b_1	middle point of back surface of HP_1	m_3	middle position of top surface of HP_3
c_1	lower point of back surface of HP_1	m_4	middle position of top surface of IP

Figure 1. (a) the experimental setup and (b) top view of the room and schematic diagram of studied cases

Figure 2. (a) the experimental setup and (b) schematic diagram of sampling position

Figure 3. Bioaerosol distributions on sampling points of case 2 in which H = 0 cm, D = 50 cm with gaspers closed. (a) detailed viable virus distribution, (b) viable virus distribution on six sub-areas, (c) comparison of HP_1 and HP_2, and (d) detailed droplet number distribution.

Figure 4. Viable virus distribution on seats under four relative heights of the backrest. Other parameters: D = 50 cm, V = 0 m/s, IP's and HP's gaspers were closed.

Figure 5. Effect of the relative height of backrest on virus deposition at areas of back surface (BS_1, BS_2), top surface (TS_1, TS_2), and head (HS_1, HS_2). PFU value was normalized by the PFU at corresponding area of case 2 with height of 0 cm.

Figure 6. Effect of relative distance of two rows on normalized PFU at areas of back surface (BS_1, BS_2), top surface (TS_1, TS_2), and head (HS_1, HS_2). PFU value was normalized by the PFU at corresponding area of case 2 with distance of 50 cm.

Figure 7. Viable virus number concentration and distribution on nearby seats under the 'open' or 'closed' status of gasper. Other parameters: H = 0 cm, D = 50 cm, V = 1.5 m/s, and gasper jet was above passenger's face.

Figure 8. Effect of status of IP's and HP's gasper jet on normalized PFU at areas of back surface (BS_1, BS_2), top surface (TS_1, TS_2), and head (HS_1, HS_2). PFU value was normalized by the PFU at corresponding area of case 2 with IP's and HP's gasper closed.

Figure 9. Effect of position of IP's gasper on normalized PFU at areas of back surface (BS_1, BS_2), top surface (TS_1, TS_2), and head (HS_1, HS_2). PFU value was normalized by the PFU at corresponding area of case 2 with IP's and HP's gasper closed.

Figure 10. Effect of velocity of IP's gasper jet on normalized PFU at areas of back surface (BS_1, BS_2), top surface (TS_1, TS_2), head (HS_1, HS_2) of HP1 and HP2. PFU value was normalized by the PFU at corresponding area of case 2 with IP's gasper being closed.

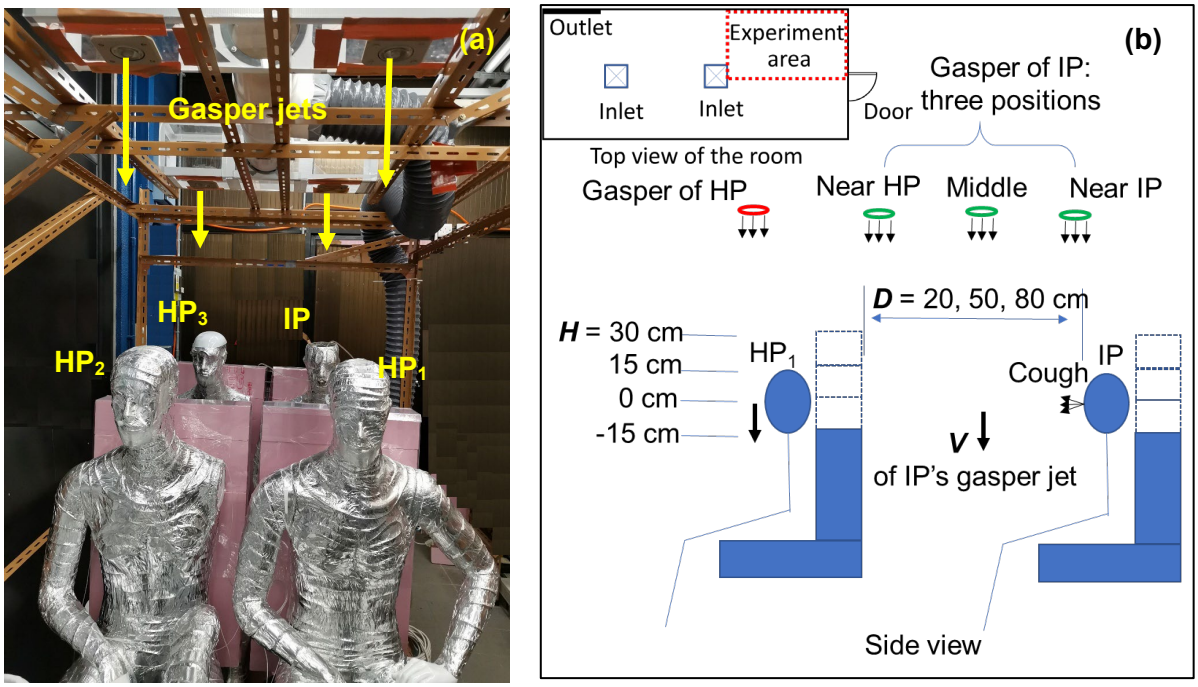

Figure 1. (a) the experimental setup and (b) top view of the room and schematic diagram of studied cases

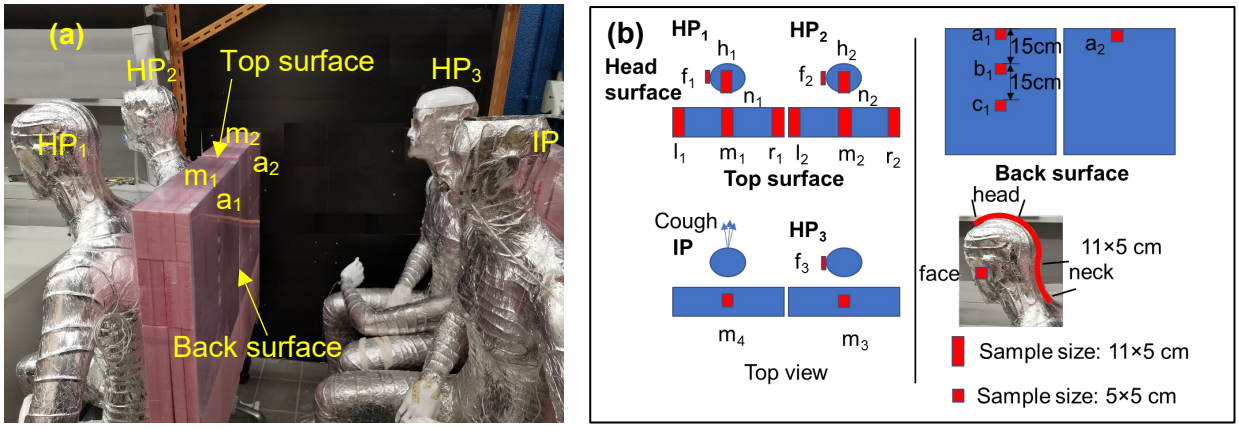

Figure 2. (a) the experimental setup and (b) schematic diagram of sampling position

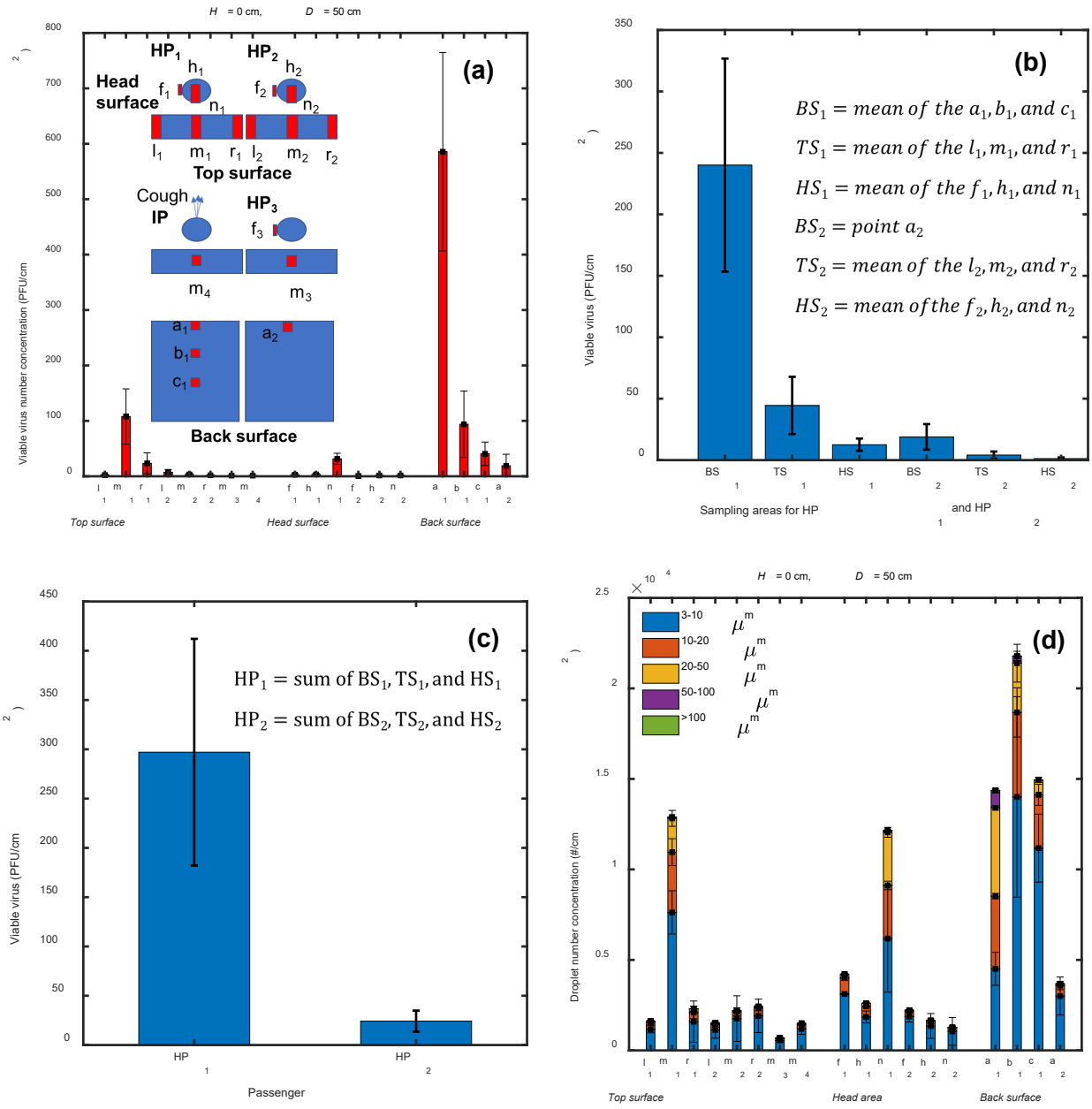

Figure 3. Bioaerosol distributions on sampling points of case 2 in which $H = 0$ cm, $D = 50$ cm with gaspers closed. (a) detailed viable virus distribution, (b) viable virus distribution on six sub-areas, (c) comparison of HP_1 and HP_2, and (d) detailed droplet number distribution.

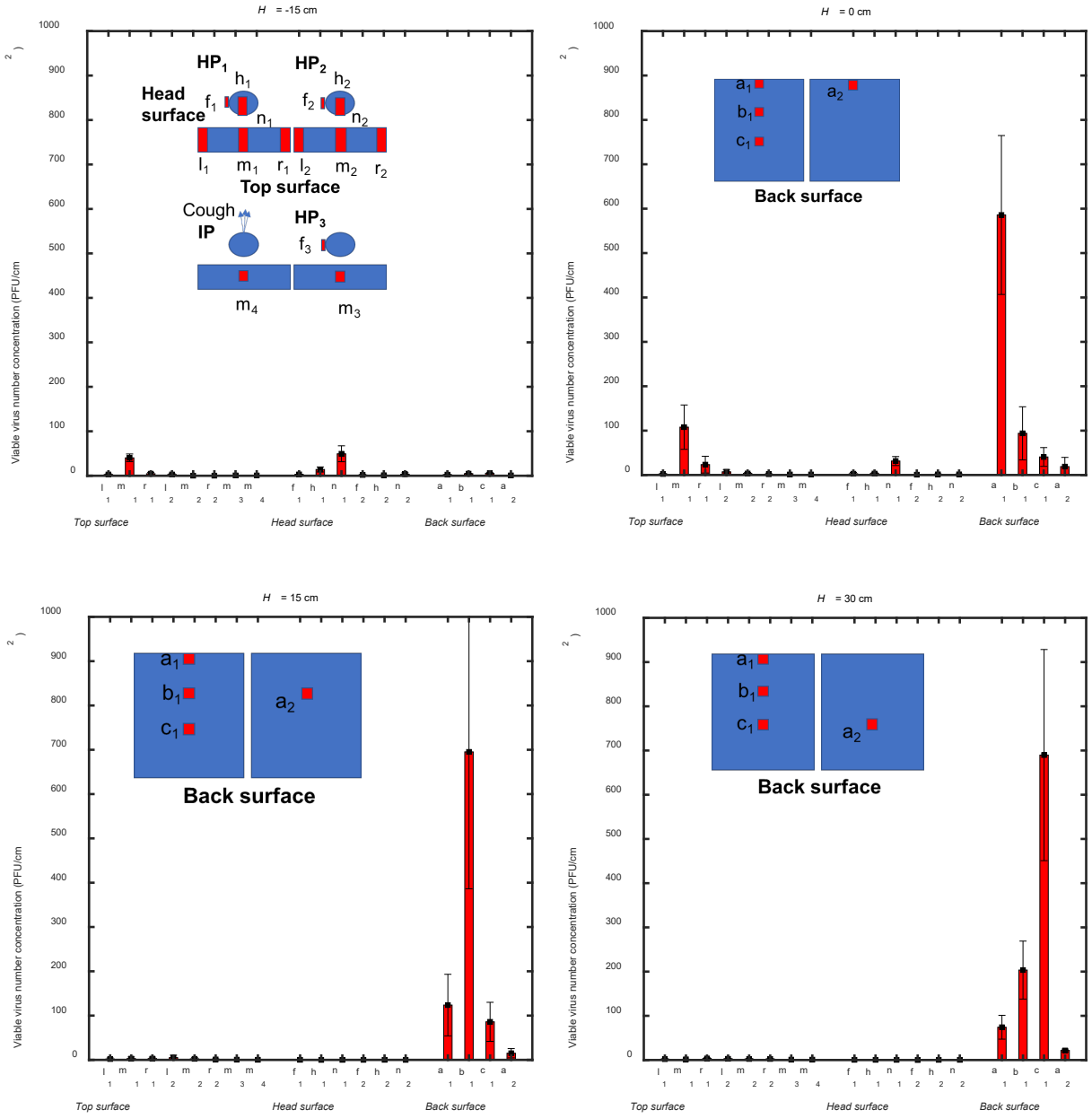

Figure 4. Viable virus distribution on seats under four relative heights of the backrest. Other parameters: D = 50 cm, V = 0 m/s, IP's and HP's gaspers were closed.

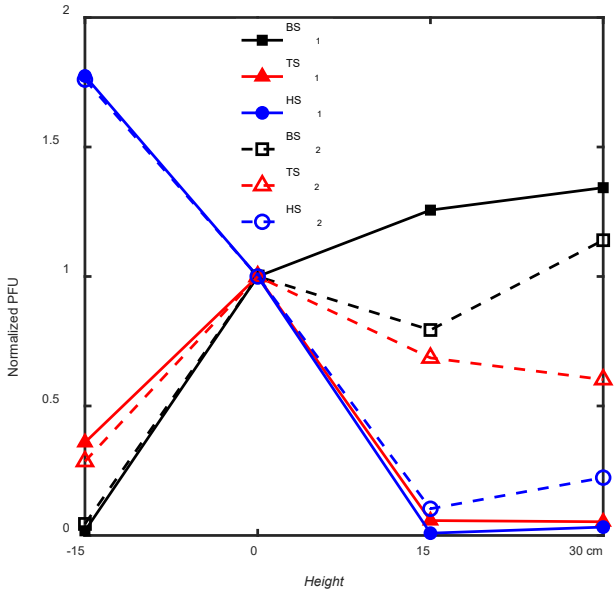

Figure 5. Effect of the relative height of backrest on virus deposition at areas of back surface (BS_1, BS_2), top surface (TS_1, TS_2), and head (HS1, HS_2). PFU value was normalized by the PFU at corresponding area of case 2 with height of 0 cm.

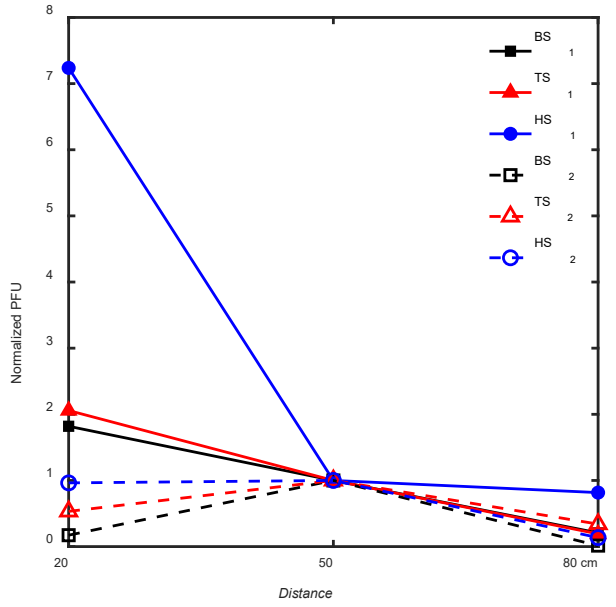

Figure 6. Effect of relative distance of two rows on normalized PFU at areas of back surface (BS_1, BS_2), top surface (TS_1, TS_2), and head (HS_1, HS_2). PFU value was normalized by the PFU at corresponding area of case 2 with distance of 50 cm.

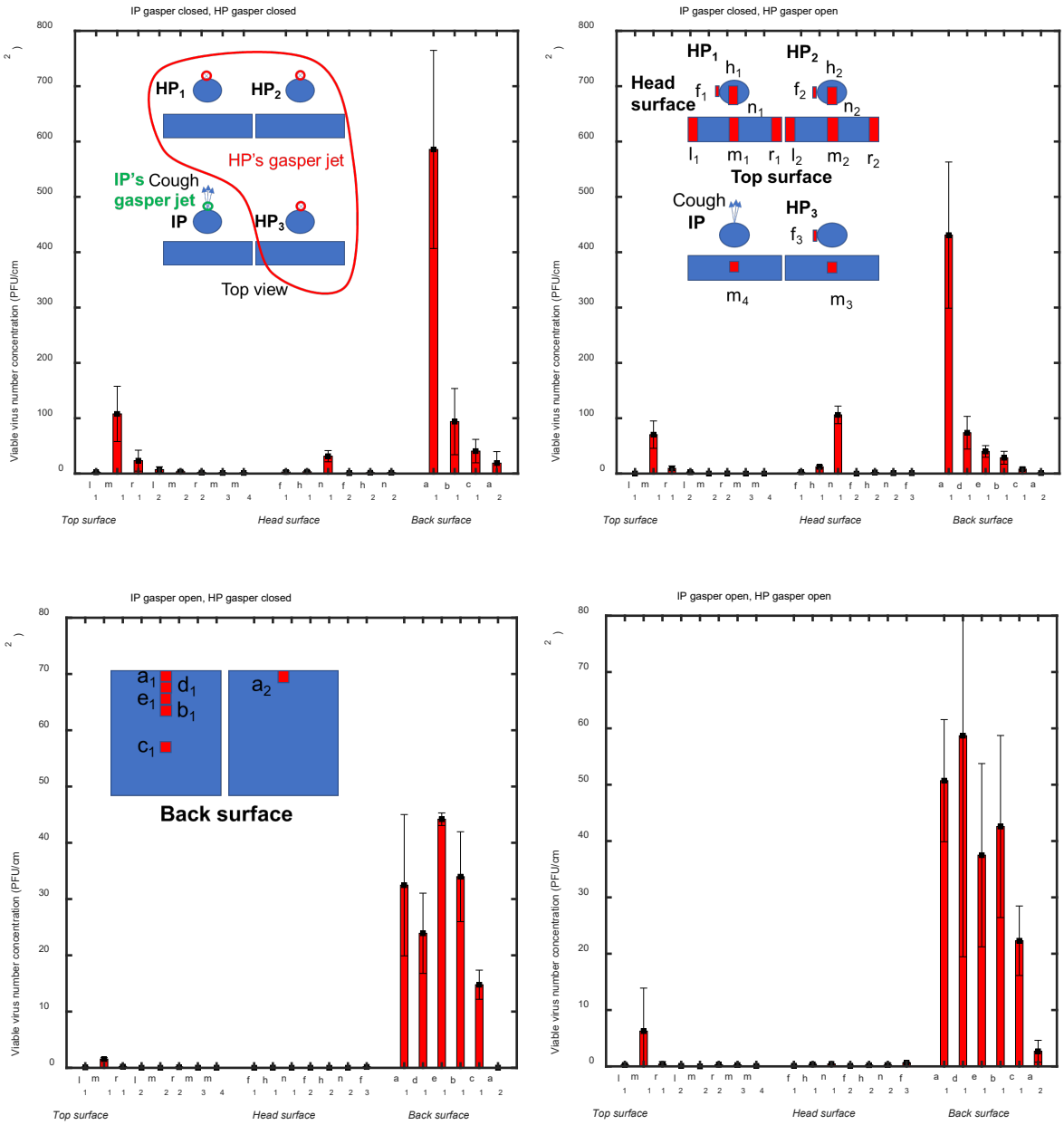

Figure 7. Viable virus number concentration and distribution on nearby seats under the 'open' or 'closed' status of gasper. Other parameters: $H = 0$ cm, $D = 50$ cm, $V = 1.5$ m/s, and gasper jet was above passenger's face.

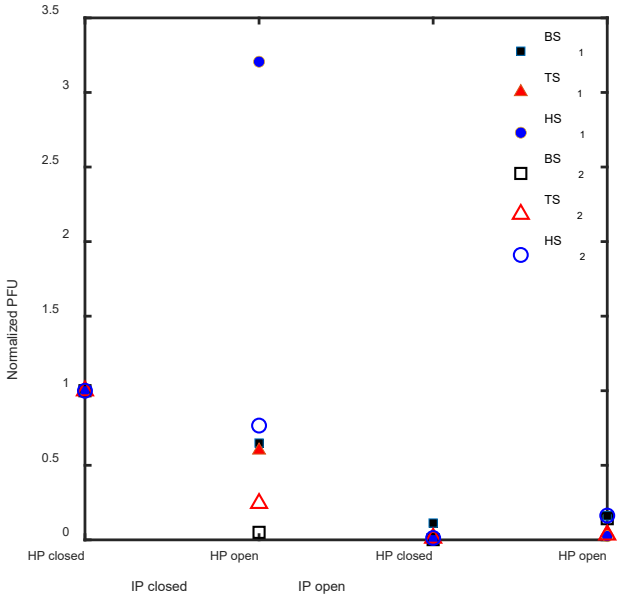

Figure 8. Effect of status of IP's and HP's gasper jet on normalized PFU at areas of back surface (BS_1, BS_2), top surface (TS_1, TS_2), and head (HS_1, HS_2). PFU value was normalized by the PFU at corresponding area of case 2 with IP's and HP's gasper closed.

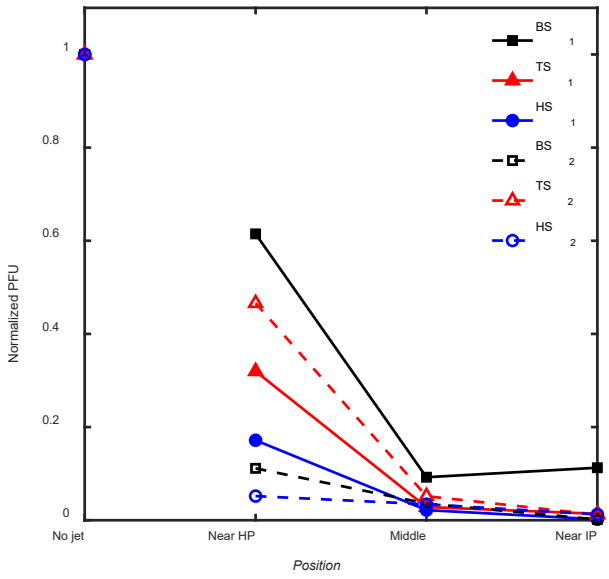

Figure 9. Effect of position of IP's gasper on normalized PFU at areas of back surface (BS_1, BS_2), top surface (TS_1, TS_2), and head (HS_1, HS_2). PFU value was normalized by the PFU at corresponding area of case 2 with IP's and HP's gasper closed.

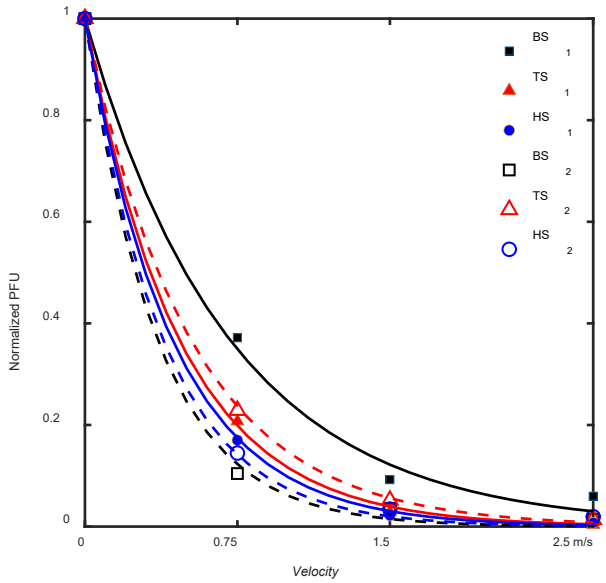

Figure 10. Effect of velocity of IP's gasper jet on normalized PFU at areas of back surface (BS_1, BS_2), top surface (TS_1, TS_2), head (HS_1, HS_2) of HP_1 and HP_2. PFU value was normalized by the PFU at corresponding area of case 2 with IP's gasper being closed.